ARMY RESEARCH LABORATORY

Predicting the Nonlinear Response and Progressive Failure of Composite Laminates

Travis A. Bogetti, Christopher P. R. Hoppel, Vasyl M. Harik, James F. Newill, and Bruce P. Burns

ARL-RP-75 **June 2004**

A reprint from *Composites Science and Technology*, 2004, *64*, 329–342.

NOTICES

Disclaimers

The findings in this report are not to be construed as an official Department of the Army position unless so designated by other authorized documents.

Citation of manufacturer's or trade names does not constitute an official endorsement or approval of the use thereof.

Destroy this report when it is no longer needed. Do not return it to the originator.

Army Research Laboratory
Aberdeen Proving Ground, MD 21005-5069

ARL-RP-75 **June 2004**

Predicting the Nonlinear Response and Progressive Failure of Composite Laminates

Travis A. Bogetti, Christopher P. R. Hoppel, Vasyl M. Harik, James F. Newill, and Bruce P. Burns
Weapons and Materials Research Directorate, ARL

A reprint from *Composites Science and Technology*, 2004, *64*, 329–342.

Report Documentation Page

Form Approved
OMB No. 0704-0188

1. REPORT DATE *(DD-MM-YYYY)*	2. REPORT TYPE	3. DATES COVERED (From - To)
June 2004	Reprint	December 1998–June 1999

4. TITLE AND SUBTITLE
Predicting the Nonlinear Response and Progressive Failure of Composite Laminates

5a. CONTRACT NUMBER

5b. GRANT NUMBER

5c. PROGRAM ELEMENT NUMBER

6. AUTHOR(S)
Travis A. Bogetti, Christopher P. R. Hoppel, Vasyl M. Harik, James F. Newill, and Bruce P. Burns

5d. PROJECT NUMBER
622618.AH80

5e. TASK NUMBER

5f. WORK UNIT NUMBER

7. PERFORMING ORGANIZATION NAME(S) AND ADDRESS(ES)
U.S. Army Research Laboratory
ATTN: AMSRD-ARL-WM-MB
Aberdeen Proving Ground, MD 21005-5069

8. PERFORMING ORGANIZATION REPORT NUMBER
ARL-RP-75

9. SPONSORING/MONITORING AGENCY NAME(S) AND ADDRESS(ES)
OPM-TMAS
Picatinny Aresenal, NJ 07806-5000

10. SPONSOR/MONITOR'S ACRONYM(S)

11. SPONSOR/MONITOR'S REPORT NUMBER(S)

12. DISTRIBUTION/AVAILABILITY STATEMENT
Approved for public release; distribution is unlimited.

13. SUPPLEMENTARY NOTES
A reprint from *Composites Science and Technology*, 2004, *64*, 329–342.

14. ABSTRACT
A comprehensive comparison of laminate failure models was established to assess the state-of-the-art in laminate modeling technologies on an international level (known as Worldwide Failure Olympics Exercise) [1]. This report represents one contribution (Part A) to the Exercise, where predictions for laminate response and failure behavior of various laminates under a broad range of loading conditions are made. A method for predicting the nonlinear stress/strain response and failure behavior of composite laminates is described. Predictions are based on an incremental formulation of a well-established three-dimensional laminated media analysis [2] coupled with a progressive-ply failure methodology. Nonlinear lamina constitutive relations for the composites are represented using the Ramberg-Osgood equation [3]. Piece-wise linear increments in laminate stress and strain are calculated and superimposed to formulate the overall effective nonlinear response. Individual ply stresses and strain are monitored to calculate instantaneous ply stiffnesses for the incremental solution and to establish ply failure levels. The progressive-ply failure approach allows for stress unloading in a ply and discrimination of the various potential modes of failure. Laminate response and failure predictions for 14 different cases are presented. The cases include prediction of the effective nonlinear stress vs. strain responses of laminates, as well as, initial and final ply failure envelope predictions under multi-axial loading. Comparison of predictions with actual experimental data will be made in a companion report to be published in Part B of the Exercise.

15. SUBJECT TERMS
composite, laminate, progressive failure, mechanical response, nonlinear, failure mode, LAM3D-NL

16. SECURITY CLASSIFICATION OF:			17. LIMITATION OF ABSTRACT	18. NUMBER OF PAGES	19a. NAME OF RESPONSIBLE PERSON
a. REPORT	b. ABSTRACT	c. THIS PAGE			Travis A. Bogetti
UNCLASSIFIED	UNCLASSIFIED	UNCLASSIFIED	UL	32	19b. TELEPHONE NUMBER (*Include area code*) 410-306-0859

Standard Form 298 (Rev. 8/98)
Prescribed by ANSI Std. Z39.18

Available online at www.sciencedirect.com
SCIENCE DIRECT®
Composites Science and Technology 64 (2004) 329–342
COMPOSITES SCIENCE AND TECHNOLOGY
www.elsevier.com/locate/compscitech

Predicting the nonlinear response and progressive failure of composite laminates

Travis A. Bogetti*, Christopher P.R. Hoppel, Vasyl M. Harik, James F. Newill, Bruce P. Burns

US Army Research Laboratory; AMSRL-WM-MB, Aberdeen Proving Ground, MD 21005-5066, USA

Received 1 October 1998; accepted 1 November 2001

Abstract

A comprehensive comparison of laminate failure models was established to assess the state-of-the-art in laminate modeling technologies on an international level (known as the Worldwide Failure Olympics Exercise) [1]. This paper represents one contribution (Part A) to the Exercise, where predictions for laminate response and failure behavior of various laminates under a broad range of loading conditions are made. A method for predicting the nonlinear stress/strain response and failure behavior of composite laminates is described. Predictions are based on an incremental formulation of a well-established three-dimensional laminated media analysis [2] coupled with a progressive-ply failure methodology. Nonlinear lamina constitutive relations for the composites are represented using the Ramberg–Osgood equation [3]. Piece-wise linear increments in laminate stress and strain are calculated and superimposed to formulate the overall effective nonlinear response. Individual ply stresses and strains are monitored to calculate instantaneous ply stiffnesses for the incremental solution and to establish ply failure levels. The progressive-ply failure approach allows for stress unloading in a ply and discrimination of the various potential modes of failure. Laminate response and failure predictions for 14 different cases are presented. The cases include prediction of the effective nonlinear stress-vs.-strain responses of laminates, as well as, initial and final ply failure envelope predictions under multi-axial loading. Comparison of predictions with actual experimental data will be made in a companion paper to be published in Part B of the Exercise.
Published by Elsevier Ltd.

Keywords: Composite laminate

1. Introduction

1.1. Background

Predicting the mechanical response and failure behavior of laminated composites is vitally important for efficient design in structural applications. Few would argue that predicting the effective laminate strain response to mechanical load is far easier than predicting the failure (or post failure) behavior of the laminate. It is not surprising that this subject has received a great wealth of attention since the early days of composite mechanics.

Many different approaches exist for laminate failure analysis with varied complexity and successes. Surveys abound on the subject: Chamis [4], Sandhu [5], Soni [6], Tsai [7], and Nahas [8]. Review of the literature reveals the broad spectrum of approaches that are employed in laminate failure prediction. With such a broad range of approaches, predictions for particular laminate configurations and loading are also likely to be widely varied.

To address this issue, a recent effort has been launched by Hinton and Soden [1] to assess the state-of-the-art in prediction capabilities for laminate response and failure. This effort requested originators of a variety of laminate failure theories to make performance predictions of specific carbon- and glass-fiber-reinforced epoxy laminates subjected to a range of biaxial loads, using the same given material properties, laminate arrangements, and loading conditions. Each of the contributors has submitted a paper documenting their predictions for 14 different laminate cases including a report on their respective failure theory and approach [9–20]. Specifics of the exercise are published in a separate report [21]. The predictions submitted by the con-

* Corresponding author.

0266-3538/$ - see front matter Published by Elsevier Ltd.
doi:10.1016/S0266-3538(03)00217-3

tributors have been compared, and differences in their respective approaches have been identified and discussed [22]. For the most part, the submitted laminate predictions for stresses and strains are based on classical laminated plate theory or a similar derivative while laminate failure behavior is modeled with a wider variety of approaches.

This paper represents our laminate response and failure predictions to the 14 laminate cases described in Part A of the Exercise [1]. Subsequently, we plan to participate in Part B of the Exercise and compare our predictions with the experimental data.

1.2. Current approach

The approach taken in our investigation is based on the three-dimensional laminated media analysis presented by Chou et al. [2]. This analysis is similar to Classical Laminated Plate Theory (CLPT) except that through thickness stresses and strains are accounted for in the formulation. Additionally, laminate curvatures are not a permitted type of deformation, which makes this theory more relevant to thick laminated composite analysis. As with CLPT, ply stresses and strains are calculated from applied average stress resultant type mechanical loads. In-plane laminate behavior and ply stress and strain predictions for this theory are nearly identical to those made by CLPT for laminates which possess balanced and symmetric lay-ups—those which do not possess bending-twisting-coupling modes of deformation. Specific details of the analysis are highlighted in the Analysis section of this paper. All of the 14 laminates cases studied in this exercise posses balanced and symmetric architectures.

The laminated media analysis technique presented by Chou et al. [2] was used for predicting linear-elastic material response and failure in composite laminates [23]. In the present study, we have extended this capability to predict nonlinear material behavior by adopting a piece-wise linear incremental approach. Essentially, the effective nonlinear laminate stress/strain response predictions are determined from the superposition of piece-wise linear segments in stress and strain during an incremental loading scheme. The individual ply stresses and strains are computed at each step during the incremental loading history. The effective laminate stiffness matrix is updated at each load increment and is based on strain-dependent tangent ply properties.

Progressive laminate failure is modeled with a maximum strain-based ply failure criteria and a ply modulus discount method. When a strain allowable in any ply is reached during the incremental laminate loading, the associated modulus to the particular failure mode is reduced and the corresponding load is subsequently redistributed within in the laminate. Incremental loading is continued until the laminate cannot sustain load without undergoing excessive deformation or strain. Details of the laminated media analysis, the piece-wise linear incremental loading strategy, and the progressive ply failure methodology are described in the following section.

2. Analysis

2.1. Three-dimensional laminate media analysis

In this work, the analytic model developed by Chou et al. [2] is used to predict the effective laminate stress/strain response. It is also used to calculate ply-level stresses and strains during incremental loading for failure and strength prediction [23]. The following section outlines the laminated media model upon which our analysis is based.

Chou et al. [2] use a control volume approach to yield a closed-form solution to the problem of effective homogeneous property determination for a laminated media composed of individual layers. Unlike the works of White and Angona [24], Postma [25], Rytov [26], Behrens [27], and Salamon [28], which required the individual layers to be isotropic, Chou et al. [2] permitted general anisotropy of the layers. The analysis is based on the assumptions that all interlaminar stresses are continuous across ply interfaces and that all in-plane strains are continuous through the thickness dimension of a representative volume element (i.e., a repeating sublaminate configuration).

The following expression is used to represent the effective (i.e., homogeneous) stress/strain constitutive relationship for an N-layered laminate (see Fig. 1):

$$\overline{\sigma_i^*} = \overline{C_{ij}^*}\,\overline{\varepsilon_j^*} \text{ for } (i,j = 1,2,3,4,5,6). \tag{1}$$

The barred notation is used to denote that the relationship applies in the global x–y–z coordinate system of the laminate. The asterisk superscript is used here to denote the "average" or effective laminate stress and strain quantities. In-plane strains are assumed uniform (i.e.,

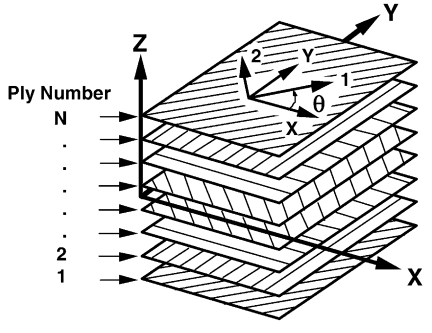

Fig. 1. Laminate configuration.

constant within each ply) and equal to the effective strains of the laminate. Mathematically, this is expressed as

$$\overline{\varepsilon_i^k} = \overline{\varepsilon_i^*} \text{ for } (i = 1, 2, 6; k = 1, 2, \ldots, N), \tag{2}$$

where $\overline{\varepsilon_i^k}$ represents the strain in the kth ply of the laminate (see ply numbering convention in Fig. 1). To ensure stress continuity across ply interfaces, all ply stress components associated with the out-of-plane direction (i.e., z-direction) are assumed uniform and equal to the corresponding effective stresses in the laminate. Mathematically, this is expressed as

$$\overline{\sigma_i^k} = \overline{\sigma_i^*} \text{ for } (i = 3, 4, 5; k = 1, 2, \ldots, N), \tag{3}$$

where $\overline{\sigma_i^k}$ represents the stress in the kth ply of the laminate.

All remaining effective laminate strains and stresses are assumed to be the volume average of all their corresponding ply strain and stress components, respectively. Mathematically, these assumptions are expressed as

$$\overline{\varepsilon_i^*} = \sum_{k=1}^{N} V^k \overline{\varepsilon_i^k} \text{ for } (i = 3, 4, 5) \tag{4}$$

and

$$\overline{\sigma_i^*} = \sum_{k=1}^{N} V^k \overline{\sigma_i^k} \text{ for } (i = 1, 2, 6), \tag{5}$$

where V^k is the ratio of the original (i.e., undeformed) volume of the kth ply over the original volume of the entire laminate. The constitutive equation for each ply in the laminate is written below [Eq. (6)] using the superscript notation.

$$\overline{\sigma_i^k} = \overline{C_{ij}^k \varepsilon_j^k} \text{ for } (i, j = 1, 2, 3, 4, 5, 6; k = 1, 2, \ldots, N). \tag{6}$$

(For completeness, the ply stiffness matrix coefficients ($\overline{C_{ij}^k}$) are defined in terms of the lamina engineering constants and layer orientations in the Appendix)

Eqs. (1)–(6) represent 12N + 6 linear algebraic equations with 12N + 12 unknowns. Solution to Eqs. (1)–(6) yields the following effective three-dimensional stress/strain constitutive relation, which can be used as an equivalent (i.e., homogeneous) representation for the laminated media where the coefficients in the laminate stiffness matrix, $\overline{C_{ij}^k}$, are given by

$$\overline{C_{ij}^*} = \sum_{k=1}^{N} V^k \left[\overline{C_{ij}^k} - \frac{\overline{C_{13}^k C_{3j}^k}}{\overline{C_{33}^k}} + \frac{\overline{C_{i3}^k} \sum_{\ell=1}^{N} \frac{V^\ell \overline{C_{3j}^k}}{\overline{C_{33}^k}}}{\overline{C_{33}^k} \sum_{\ell=1}^{N} \frac{V^\ell}{\overline{C_{33}^k}}} \right] \text{for } (i, j = 1, 2, 3, 6), \tag{7}$$

$$\overline{C_{ij}^*} = \overline{C_{ji}^*} = 0 \text{ for } (i = 1, 2, 3, 6; j = 4, 5) \tag{8}$$

and

$$\overline{C_{ij}^*} = \left[\frac{\sum_{k=1}^{N} \frac{V^k}{\Delta_k} \overline{C_{ij}^k}}{\sum_{k=1}^{N} \sum_{\ell=1}^{N} \frac{V^k V^\ell}{\Delta_k \Delta_\ell} \left(\overline{C_{44}^k C_{55}^k} - \overline{C_{45}^k C_{54}^k} \right)} \right] \text{for } (i, j = 4, 5), \tag{9}$$

where

$$\Delta_k = \begin{vmatrix} \overline{C_{44}^k} & \overline{C_{45}^k} \\ \overline{C_{54}^k} & \overline{C_{55}^k} \end{vmatrix} = \overline{C_{44}^k}\ \overline{C_{55}^k} - \overline{C_{45}^k}\ \overline{C_{54}^k}. \tag{10}$$

The effective stress/strain constitutive relation for the laminated media is therefore given by Eqs. (1) and (7)–(10).

In determining the individual ply-level stresses and strains, the assumption is made that the applied mechanical loading on the laminated media ($\overline{\sigma_i^*}$) is known, uniform, and represents the 'average' or 'effective' stress acting on the sublaminate configuration. The associated "effective" or "smeared" laminate strains ($\overline{\varepsilon_i^*}$) can be obtained directly from the inversion of Eq. (1). From the assumption made in Eq. (2), all in-plane strain values (defined in the global x–y–z coordinate system) for plies 1 through N are therefore known. Similarly, from the assumption made in Eq. (2), all out-of-plane stresses for plies 1 through N are known (also defined in the global x–y–z coordinate system). The out-of-plane ply strains and in-plane ply stresses remain to be determined.

Sun and Liao [29] derived the following expression for determination of the remaining out-of plane ply strains

$$\begin{bmatrix} \overline{\varepsilon_3^k} \\ \overline{\varepsilon_4^k} \\ \overline{\varepsilon_5^k} \end{bmatrix} = \begin{bmatrix} \overline{C_{33}^k C_{34}^k C_{35}^k} \\ \overline{C_{43}^k C_{44}^k C_{45}^k} \\ \overline{C_{53}^k C_{54}^k C_{55}^k} \end{bmatrix}^{-1} \left[\begin{bmatrix} \overline{\sigma_3^k} \\ \overline{\sigma_4^k} \\ \overline{\sigma_5^k} \end{bmatrix} - \begin{bmatrix} \overline{C_{31}^k C_{32}^k C_{36}^k} \\ \overline{C_{41}^k C_{42}^k C_{46}^k} \\ \overline{C_{51}^k C_{52}^k C_{56}^k} \end{bmatrix} \begin{bmatrix} \overline{\varepsilon_1^k} \\ \overline{\varepsilon_2^k} \\ \overline{\varepsilon_6^k} \end{bmatrix} \right]. \tag{11}$$

Once all of the ply strains are known, the remaining in-plane ply stresses can be calculated straightforwardly through the following relation

$$\begin{bmatrix} \overline{\sigma_1^k} \\ \overline{\sigma_2^k} \\ \overline{\sigma_6^k} \end{bmatrix} = \begin{bmatrix} \overline{C_{11}^k C_{12}^k C_{13}^k C_{14}^k C_{15}^k C_{16}^k} \\ \overline{C_{21}^k C_{22}^k C_{23}^k C_{24}^k C_{25}^k C_{26}^k} \\ \overline{C_{61}^k C_{62}^k C_{63}^k C_{64}^k C_{65}^k C_{66}^k} \end{bmatrix} \begin{bmatrix} \overline{\varepsilon_1^k} \\ \overline{\varepsilon_2^k} \\ \overline{\varepsilon_3^k} \\ \overline{\varepsilon_4^k} \\ \overline{\varepsilon_5^k} \\ \overline{\varepsilon_6^k} \end{bmatrix}. \tag{12}$$

2.2. Defining nonlinear lamina constitutive relations

Material nonlinearity in our laminate analysis is accounted for on the lamina or ply level. The nonlinear

lamina constitutive relations (i.e., stress-vs.-strain relations) for each of the principal lamina directions are defined with the Ramberg–Osgood equation [3]. For the treatment of unidirectional lamina in our three-dimensional analysis, this would include the fiber direction (1), in-plane transverse direction (2), transverse normal direction (3), interlaminar shear directions (23 and 13), and the in-plane shear direction (12).

The Ramberg–Osgood equation provides an expression for stress written explicitly in terms of strain and three unique parameters,

$$\sigma = \frac{E_o \varepsilon}{\left(1 + \left(\frac{E_o \varepsilon}{\sigma_o}\right)^n\right)^{\frac{1}{n}}}. \tag{13}$$

here E_o is the initial modulus, σ_o is the asymptotic stress level, and n is a shape parameter for the stress versus strain curve. Fig. 2 graphically illustrates the significance of these parameters with a typical nonlinear stress-vs.-strain relationship.

For computational considerations, it is desired to define the instantaneous or tangent lamina stiffness as a continuous function of strain. Taking the derivative of Eq. (13) with respect to strain, the following expression is obtained:

$$E_t = \frac{d\sigma}{d\varepsilon} = \frac{E_o}{\left(1 + \left(\frac{E_o \varepsilon}{\sigma_o}\right)^n\right)^{1+\frac{1}{n}}}, \tag{14}$$

where E_t is the instantaneous or tangent lamina stiffness modulus expressed explicitly in terms of strain and the three Ramberg–Osgood parameters.

A unique set of Ramberg–Osgood parameters for each of the principal directions in the lamina is required. A fitting routine was implemented to find the Ramberg–Osgood parameters which realistically represent the stress/strain response for each of the four materials used in the study. As an example, the data fit to Eq. (13) is illustrated in Fig. 3 for the nonlinear 12-shear direction stress/strain response of the E-glass/MY750 material. A full account of all the Ramberg–Osgood parameters used in our analysis is provided in the Results section of this paper.

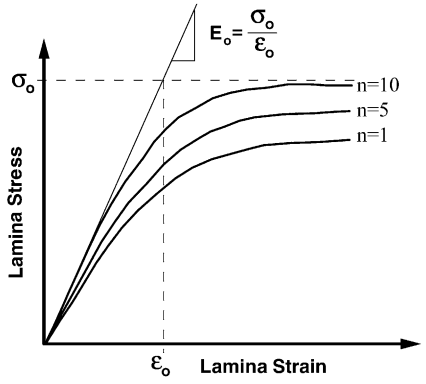

Fig. 2. Ramberg–Osgood parameters definitions.

2.3. Incremental approach (solution strategy)

The nonlinear response of the laminate is generated through the summation of piece-wise linear increments in stress over a pre-established load schedule. An incremental form of Eq. (1) is used to determine the linear increments in laminate stress-and-strain. The laminate stiffness matrix is updated at the end of each stress increment (based on all current ply strain levels) during the incremental loading strategy. The schematic presented in Fig. 4 provides a mathematical representation of the incremental loading strategy for an arbitrary laminate.

Assume that at point (a), corresponding to the end of the *nth* stress increment, the strain and stress state of the laminate is known ($\overline{\varepsilon^*}_j^n$, $\overline{\sigma^*}_i^n$). From this point, the objective is to determine the strain and stress state at point (b) or ($\overline{\varepsilon^*}_j^{n+1}$, $\overline{\sigma^*}_i^{n+1}$). The effective laminate stiffness matrix at the end of stress increment n, $\overline{C^*_{ij}}^n$, is computed from an incremental form of the laminated media model constitutive relation, Eq. (1). With the increment in load defined, $\Delta\overline{\sigma^*}_i^n$, the corresponding increment in laminate strain, $\Delta\overline{\varepsilon^*}_j^n$, is calculated from an inverse form of Eq. (1):

$$\Delta\overline{\varepsilon}_i^* = \left[\overline{C_{ij}^*}\right]^{-1} \Delta\overline{\sigma}_i^*, \quad (i, j = 1, 2, 3, 4, 5, 6). \tag{15}$$

Individual ply stress and strain increments are calculated according to the equations presented previously. A

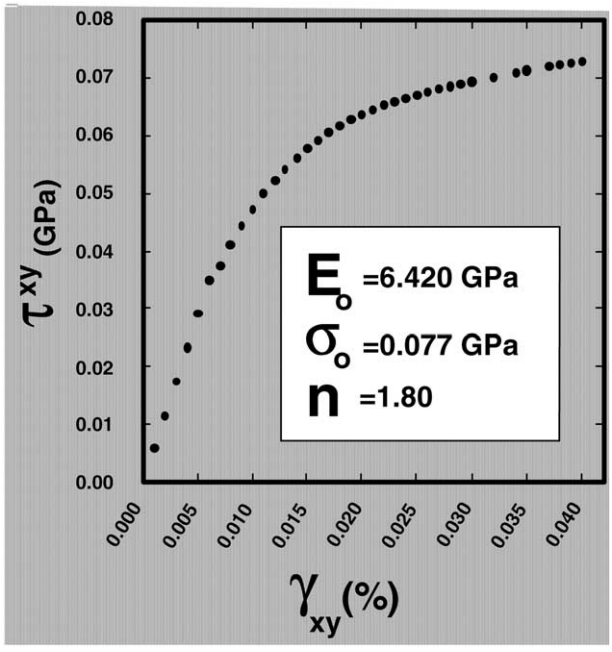

Fig. 3. Ramberg–Osgood parameters fit to E-glass/MY750 epoxy data.

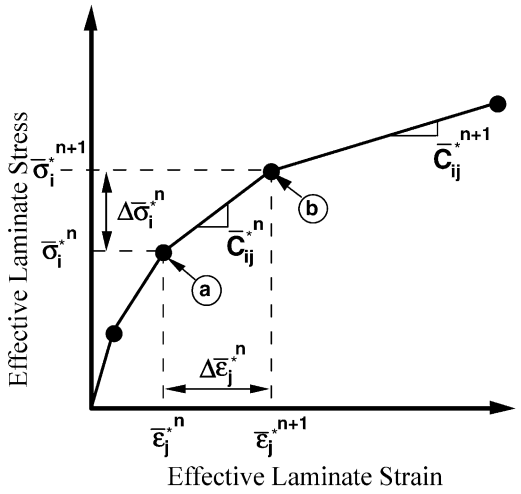

Fig. 4. Incremental laminate loading methodology.

cumulative summation is maintained to track the total stress-and-strain levels in each ply of the laminate. The tangent modulus values for each ply and material direction are calculated according to Eq. (14) and used in the determination of the laminate stiffness matrix for the next laminate stress increment calculation.

The entire nonlinear response for the laminate is obtained by the cumulative sum of all stress and strain increments throughout the entire stress loading history. The implementation of a progressive ply failure methodology into this incremental loading strategy is described in the next section.

2.4. Lamina failure methodology

Failure of individual plies and their effect on the overall laminate response during incremental loading are accounted for in our analysis. Our ply failure predictions are based on the well-established Maximum Strain Failure Criterion [8,30]. The Maximum Strain Failure Criterion predicts that a material will fail when the strain in any direction exceeds its corresponding allowable level. The principal ply strains in the six directions (ε_1, ε_2, ε_3, ε_4, ε_5, and ε_6) are compared to their corresponding maximum strain allowables:

if $\varepsilon_1 > 0$ and if $\varepsilon_1 >$ Y1T,
then the failure mode is fiber tension, (16a)

if $\varepsilon_1 < 0$ and if $|\varepsilon_1| >$ Y1C,
then the failure mode is fiber compression, (16b)

if $\varepsilon_2 > 0$ and if $\varepsilon_2 >$ Y2T,
then the failure mode is transverse tension, (16c)

if $\varepsilon_2 < 0$ and if $|\varepsilon_2| >$ Y2C,
then the failure mode is transverse compression, (16d)

if $\varepsilon_3 > 0$ and if $\varepsilon_3 >$ Y3T,
then the failure mode is transverse tension, (16e)

if $\varepsilon_3 < 0$ and if $|\varepsilon_3| >$ Y3C,
then the failure mode is transverse compression, (16f)

if $|\varepsilon_4| >$ Y23,
then the failure mode is interlaminar shear, (16g)

if $|\varepsilon_5| >$ Y13,
then the failure mode is interlaminar shear, (16h)

and if $|\varepsilon_6| >$ Y12,
then the failure mode is in − plane shear. (16i)

In Eqs. (16a)–(16i), Y1T is the maximum tensile strain in the 1-direction (longitudinal), Y1C is the maximum compressive strain in the 1-direction, Y2T is the maximum tensile strain in the 2-direction (transverse), Y2C is the maximum compressive strain in the 2-direction, Y3T is the maximum tensile strain in the 3-direction (out-of-plane), Y3C is the maximum compressive strain in the 3-direction, Y23 is the maximum shear strain in the 23-plane, Y13 is the maximum shear strain in the 13-plane, and Y12 is the maximum shear strain in the 12-plane.

As the laminate is loaded and laminate strains develop, the individual ply strains are monitored. When ply failure is predicted in any ply, according to the maximum strain failure criteria, the incremental loading to that point is stopped and the entire laminate stress vs. strain response is recorded. The modulus associated with the particular mode of failure in the failed ply is then reduced to an insignificant value (as well as the associated Poisson's ratio), and the incremental loading strategy is repeated from the beginning (all stresses and strains are set to zero). The loading procedure is continued until the next failure in a ply is detected. The corresponding modulus value is again discounted, the laminate response is recorded, and the procedure is repeated. This progressive ply failure response is repeated until final failure is determined, which is assumed when the

laminate looses sufficient stiffness such that it cannot carry any load without undergoing an arbitrarily excessive amount of deformation (say greater than 5% strain).

The entire laminate response is determined by the stress vs. strain response up to the point of failure, and then the load is assumed to drop to the level of the subsequent stress vs. strain curve response. The load path then continues until failure and drops again. This methodology essentially corresponds to progressive ply failure where the load in failure plies is redistributed to adjacent plies under a displacement controlled load path history.

2.5. Thermal residual stresses

Thermal residual stresses resulting from thermal expansion mismatch in adjacent plies in the laminates during cool down from the stress-free state at the cure temperature were not accounted for in the predictions. Their actual calculation follows straightforwardly from the analysis derivation described in the previous section. For completeness, however, a full description of their determination is given elsewhere [23]. It is acknowledged that the inclusion of thermal residual stresses will have some effect on the ultimate laminate strength predictions. The exact effect, however, will depend on the specific laminate architecture and loading considered.

2.6. Analysis execution

The aforementioned laminate analysis and progressive ply failure methodology has been programmed into a FORTRAN-based software code entitled LAM3DNL. The LAM3DNL code employs a user-friendly database format for input of laminate architectures, lamina properties, and failure parameters [23]. Output from the code includes the effective laminate stress and strain files as well as a failure assessment summary file that identifies all ply failures that occur during a laminate response prediction program run.

3. Results and discussion

3.1. Test case summary

In this section, we present predictions for the 14 different laminate test cases described by Soden et al. [21]. These cases have been grouped into three classes (a) biaxial failure envelopes of unidirectional lamina, (b) bidirectional failure envelopes of multidirectional laminates, and (c) stress vs. strain curves of laminates under uniaxial and biaxial loading. For completeness, a summary of the test cases is presented in Table 1 [21,22]. It is also noted that 4 different materials were included in the study: (a) E-glass/MY750 epoxy, (b) E-glass/LY556 epoxy, (c) T300 graphite/BSL 914C epoxy, and (d) AS4 graphite/3501-6 epoxy.

3.2. Lamina properties and failure allowables

Lamina material properties and failure allowables were provided by Soden et al. [21]. Since the required three-dimensional material properties for our analysis were not available, we have made some assumptions in order to represent the through-the-thickness material response. Upon examining the data provided in [21], we have made the reasonable assumption that the longitudinal and transverse lamina responses are linear. We also assume that the material properties are transversely isotropic such that $E_3 = E_2$, $G_{13} = G_{12}$, and $\upsilon_{13} = \upsilon_{12}$. Accordingly, the interlaminar shear modulus is assumed linear according to $G_{23} = E_2/2(1+\nu_{23})$. Additionally we assume $\upsilon_{23} = 0.40$ for all materials. It is noted that the predominant source of nonlinearity in our predictions is from the 12 shear response through G_{12}.

We fit the lamina material properties to the Ramberg–Osgood equation for input into the analysis. As stated previously, the longitudinal and transverse properties were assumed linear. To capture the linear behavior with the Ramberg–Osgood equation, a linear modulus was assumed as the initial modulus parameter (E_o), an asymptotic stress level (σ_o) was assumed which is much higher than the actual strength of the material and an arbitrarily high shape factor as also used ($n = 10$). This approach ensures that a linear modulus is used during the entire incremental loading history.

The stress-vs.-strain data provided in the exercise for the shear material responses were fit to Eq. (13). A summary of all fitted Ramberg–Osgood parameters for the four materials are summarized in Table 2. Maximum strain failure allowables were also provided by Soden et al. [21] and are summarized in Table 3.

3.3. Results for selected case studies

3.3.1. Biaxial failure envelopes of unidirectional lamina (cases 1, 2, and 3)

The biaxial failure envelope predictions of unidirectional lamina of the E-glass/LY556 epoxy under transverse and shear loading (σ_y vs. τ_{xy}) are presented in Fig. 5. The typical rectangular-shaped curve results from the failure strain in each direction being assumed independent of the other directions. For this loading case, the initial and final failure envelopes coincide everywhere except in the second quadrant, where the Poisson's effects result in early transverse tensile failure occurring in the 3-direction prior to the final transverse compressive failure in the 2-direction. This is similar to the transverse tensile failures that have occurred during axial compression of $[0/+30/0/-30]_{2S}$ laminates in other studies [31].

Table 1
Details of the laminates and loading cases [22]

Loading case	Laminate lay-up	Material	Description of loading cases
1	0	E-glass/LY556/HT907/DY063	Biaxial failure stress envelope under transverse and shear loading (σ_y vs. τ_{xy})
2	0	T300/BSL914C	Biaxial failure stress envelope under longitudinal and shear loading (σ_x vs. τ_{xy})
3	0	E-glass/MY750/HY917/DY063	Biaxial failure stress envelope under long. and transverse loading (σ_y vs. σ_x)
4	90/±30/90	E-glass/LY556/HT907/DY063	Biaxial failure stress envelope (σ_y vs. σ_x)
5	90/±30/90	E-glass/LY556/HT907/DY063	Biaxial failure stress envelope (σ_x vs. τ_{xy})
6	0/±45/90	AS4/3501-6	Biaxial failure stress envelope (σ_y vs. σ_x)
7	0/±45/90	AS4/3501-6	Stress–strain curves under uniaxial tensile loading in y direction (σ_y:σ_x = 1:0)
8	0/±45/90	AS4/3501-6	Stress–strain curves for (σ_y:σ_x = 2:1)
9	±55	E-glass/MY750/HY917/DY063	Biaxial failure stress envelope (σ_y vs. σ_x)
10	±55	E-glass/MY750/HY917/DY063	Stress–strain curves under uniaxial tensile loading for (σ_y:σ_x = 1:0)
11	±55	E-glass/MY750/HY917/DY063	Stress–strain curves for (σ_y:σ_x = 2:1)
12	0/90	E-glass/MY750/HY917/DY063	Stress–strain curve under uniaxial tensile loading for (σ_y:σ_x = 0:1)
13	±45	E-glass/MY750/HY917/DY063	Stress–strain curves for (σ_y:σ_x = 1:1)
14	±45	E-glass/MY750/HY917/DY063	Stress–strain curves for (σ_y:σ_x = 1:−1)

Table 2
Ramberg–Osgood parameters for nonlinear analysis (and Poisson's ratio)

Material and its parameters	Spacial directions for constitutive modeling					
	1	2	3	12	13	23
AS4/3501-6						
E_0 (GPa)	126	11	11	6.80	6.80	3.79
σ_0 (GPa)	100	100	100	0.097	0.097	100
n	10	10	10	1.96	1.96	10
ν	–	–	–	0.28	0.28	0.40
T300/BSL914C						
E_0 (GPa)	138	11	11	5.94	5.94	3.79
σ_0 (GPa)	100	100	100	0.083	0.083	100
n	10	10	10	2.05	2.05	10
ν	–	–	–	0.28	0.28	0.40
E-glass/LY556						
E_0 (GPa)	53.5	17.7	17.7	6.36	6.36	6.10
σ_0 (GPa)	100	100	100	0.076	0.076	100
n	10	10	10	1.85	1.85	10
ν	–	–	–	0.278	0.278	0.40
E-glass/MY750						
E_0 (GPa)	45.6	16.2	16.2	6.42	6.42	5.59
σ_0 (GPa)	100	100	100	0.077	0.077	100
n	10	10	10	1.80	1.80	10
ν	–	–	–	0.278	0.278	0.40

Table 3
Maximum strain failure allowables

Material	Y1T (%)	Y1C (%)	Y2T (%)	Y2C (%)	Y3T (%)	Y3C (%)	Y23 (%)	Y13 (%)	Y12 (%)
AS4/3501-6	1.38	−1.18	0.44	−2.00	0.44	−2.00	2.00	2.00	2.00
T300/BSL914C	1.09	−0.65	0.25	−1.82	0.25	−1.82	4.00	4.00	4.00
E-glass/LY556	2.13	−1.07	0.20	−0.64	0.20	−0.64	3.80	3.80	3.80
E-glass/MY750	2.81	−1.75	0.25	−1.20	0.25	−1.20	4.00	4.00	4.00

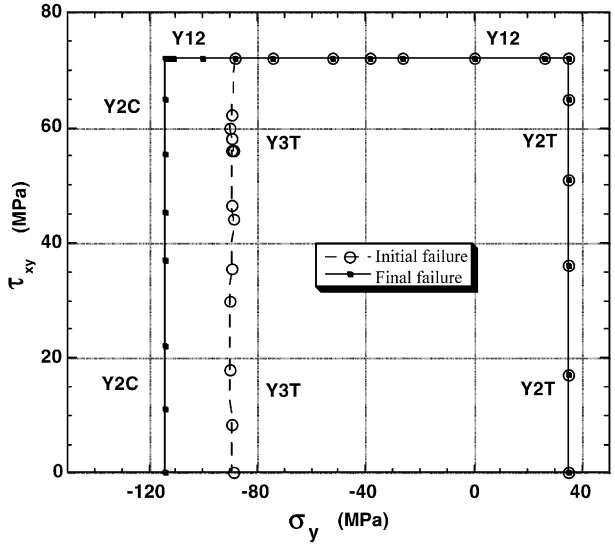

Fig. 5. Loading case 1: biaxial failure envelope (σ_y vs. τ_{xy}) and failure modes for [0] E-glass/LY556 epoxy.

The biaxial failure stress envelope for unidirectional T300/BSL914C under longitudinal and shear loading (σ_x vs. τ_{xy}) is shown in Fig. 6. Like the previous case, this case again shows a rectangular-shaped curve with shear- and axial-type failures occurring independently of other failure modes. There were no initial failures occurring prior to final fracture for this loading curve.

The biaxial failure stress envelope for loading case 3, unidirectional E-glass/MY750 under transverse and longitudinal loading (σ_y vs. σ_x), is shown in Fig. 7. For this failure case, the final tensile and compressive failures in the fiber direction (σ_x) are almost independent of the transverse stress-state. The tensile and compressive failures in the transverse (σ_y) direction are strongly influenced by the axial (σ_x) stress due to the Poisson's effects

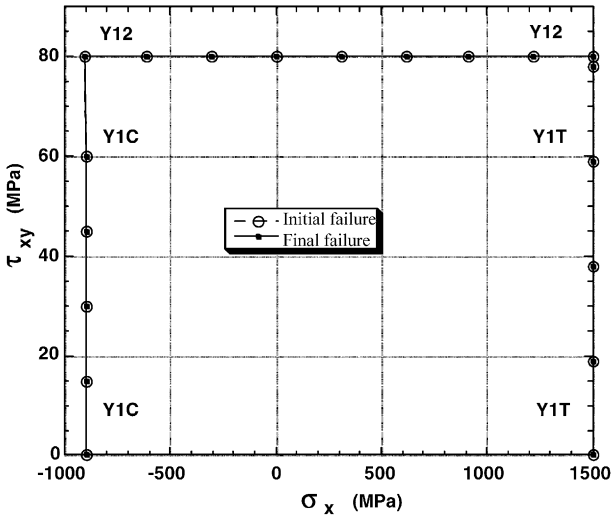

Fig. 6. Loading case 2: biaxial failure envelope of (σ_x vs. τ_{xy}) and failure modes for [0] T300 graphite/BSL 914C epoxy.

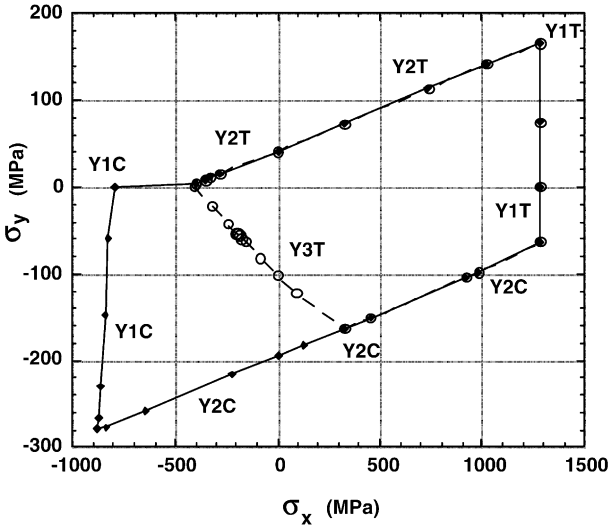

Fig. 7. Loading case 3: biaxial failure envelope of (σ_y vs. σ_x) and failure modes for [0] E-glass/MY750 epoxy.

in the material. The initial failures that are predicted in the graph are tensile failures in the 3-direction due to Poisson's effects, similar to those predicted in case 1.

3.3.2. Bidirectional failure envelopes of multi-directional laminates (cases 4–6 and 9)

For loading case 4, the biaxial failure stress envelope (σ_y vs. σ_x) of the $[90/\pm30/90]_s$ E-glass/LY556 laminate is shown in Fig. 8. For this failure envelope, the failure modes are strongly influenced by the biaxial stress-state in all directions. The laminates also experience initial failures prior to final fracture for all loading directions. Details of the progressive failure for loading case 4 are presented in Table 4.

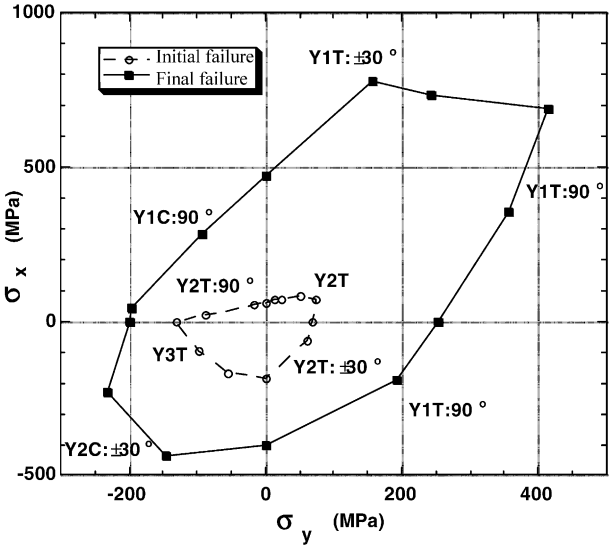

Fig. 8. Loading case 4: biaxial failure envelope (σ_y vs. σ_x) and failure modes for [90/+30/−30]s E-glass/LY556 epoxy. (See Table 4 for ply failure details.)

Table 4
Damage modes in the failure envelope for the $[90/\pm30/90]_s$ laminate shown in Fig. 8

Loading case	Damage modes	Failed plies	Stress levels (MPa)	
			σ_y	σ_x
4	Y2T	90°	0	61
Ratio:	Y1C	90°	0	474
0:1	Y2C	±30°	0	315
4	Y2T	±30°	73	73
Ratio:	Y2T	90°	91	91
1:1	Y1T	90°	357	357
4	Y2T	±30°	68	0
Ratio:	Y1T	90°	254	0
1:0	Y2C	90°	74	0
4	Y2T	±30°	61	−61
Ratio:	Y2C	90°	120	−120
1:-1	Y1T	90°	193	−193
4	Y2C	90°	0	−187
Ratio:	Y3T	all	0	−344
0:-1	Y2T	±30°	0	−383
	Y1C	±30°	0	−403
4	Y3T	all	−97	−97
Ratio:	Y2C	±30°	−231	−231
−1:-1	Y1C	90°	−192	−192
4	Y2T	90°	−132	0
Ratio:	Y3T	all	−152	0
−1:0	Y2C	±30°	−200	0
4	Y2T	90°	−89.5	21
Ratio:	Y3T	all	−170.4	40
−4.26:1	Y2C	±30°	−196.0	46

The biaxial failure envelope (σ_x vs. τ_{xy}) for the same $[90/\pm30/90]_s$ laminate of E-glass/LY556 epoxy (loading case 5) is shown in Fig. 9. Like loading case 4, the failure modes are strongly influenced by the biaxial stress-state in all directions, and the laminates also experience initial failures prior to final fracture for all of the loading directions. Details of the progressive failure for loading case 5 are presented in Table 5.

Fig. 10 shows the biaxial failure envelope (σ_y vs. σ_x) for the quasi-isotropic $[0/\pm45/90]_s$ laminate of AS4/3501-6 (loading case 6). The biaxial failure envelope (σ_y vs. σ_x) for $[+55/-55]_s$ E-glass/MY750 epoxy (loading case 9) is shown in Fig. 11. Details of the progressive failure for loading cases 6 and 9 are presented in Tables 6 and 7, respectively.

3.3.3. Stress vs. strain curves of laminates under uniaxial and biaxial loading (cases 7, 8, 10–14)

Cases 7 and 8 predict the stress-strain response of the quasi-isotropic $[0/\pm45/90]_s$ laminate of AS4/3501-6

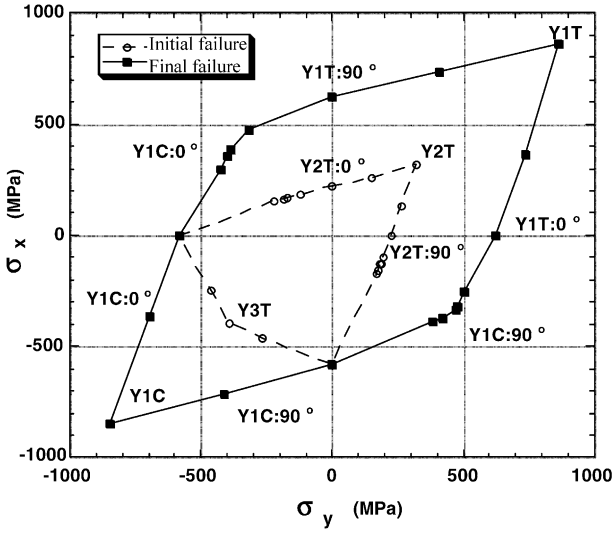

Fig. 10. Loading case 6: biaxial failure envelope (σ_y vs. σ_x) and failure modes for [0/+45/−45/90]s AS4 graphite/3501-6 epoxy. (See Table 6 for ply failure details.)

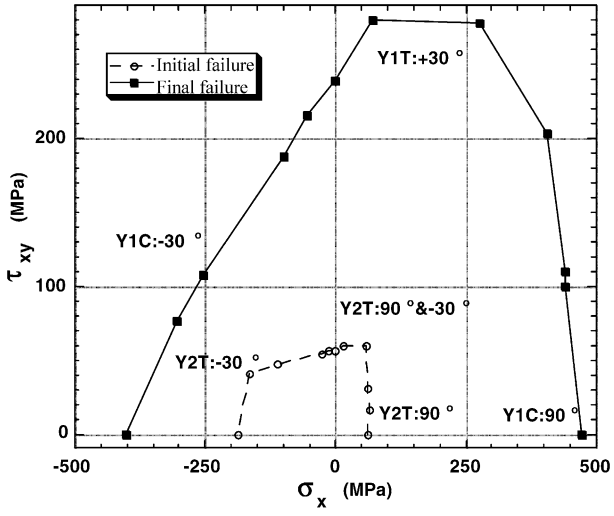

Fig. 9. Loading case 5: biaxial failure envelope of (σ_x vs. τ_{xy}) and failure modes for [90/+30/−30]s E-glass/LY556 epoxy. (See Table 5 for ply failure details.)

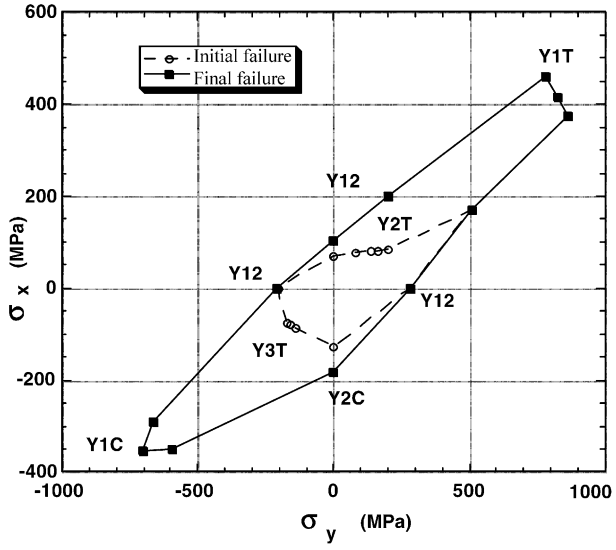

Fig. 11. Loading case 9: biaxial failure envelope (σ_y vs. σ_x) and failure modes for [+55/−55]s E-glass/MY750 epoxy. (See Table 7 for ply failure details.)

Table 5
Damage modes in the failure envelope for the $[90/\pm30/90]_s$ laminate shown in Fig. 9

Loading case	Damage modes	Failed plies	Stress levels (MPa)	
			σ_x	τ_{xy}
5	Y2T	90°	61	0
Ratio:	Y1C	90°	474	0
1:0	Y2C	±30°	311	0
5	Y2T	90°&−30°	60	60
Ratio:	Y2C	+30°	164	164
1:1	Y1T	+30°	278	278
5	Y2T	−30°	0	56
Ratio:	Y2C	+30°	0	186
0:1	Y1C	−30°	0	239
	Y2C	90°	0	45
5	Y2T	−30°	−110.4	47
Ratio:	Y2C	90°	−185.6	79
−2.35:1	Y1C	−30°	−253.8	108
5	Y2C	90°	−186	0
Ratio:	Y3T	all	−344	0
−1:0	Y2T	±30°	−383	0
	Y1C	±30°	−403	0

Table 6
Damage modes in the failure envelope for the $[0/\pm45/90]_s$ laminate shown in Fig. 10

Loading case	Damage modes	Failed plies	Stress levels (MPa)	
			σ_y	σ_x
6	Y2T	0°	0	224
Ratio:	Y2T	±45°	0	592
0:1	Y1T	90°	0	625
6	Y2T	all	318	318
Ratio:1:1	Y1T	all	860	860
6	Y2T	90°	224	0
Ratio:	Y2T	±45°	592	0
1:0	Y1T	0°	625	0
6	Y2T	90°	171	−171
Ratio:	Y12	±45°	362	−362
1:-1	Y1C	90°	386	−386
6	Y1C	90°	0	−582
Ratio:0:-1	Y2T	90°	0	−254
6	Y3T	all	−395	−395
Ratio:-1:-1	Y1C	all	−849	−849
6	Y1C	0°	−582	0
Ratio:-1:0	Y2T	0°	−254	0
6	Y2T	0°	−171	171
Ratio:	Y12	±45°	−362	362
−1:1	Y1C	0°	−386	386

used in case 6. The predictions for (σ_y:σ_x = 1:0) are shown in Fig. 12, and the predictions for (σ_y:σ_x = 2:1) are shown in Fig. 13. In both of these cases, the materials display linear behavior with several initial failures prior to the ultimate failure of the laminate.

Cases 10 and 11 predict the stress–strain response of a $[+55/-55]_s$ laminate of E-glass/MY750 epoxy. The

Table 7
Damage modes in the failure envelope for the $[\pm55]_s$ laminate shown in Fig. 11

Loading case	Damage modes	Failed plies	Stress levels (MPa)	
			σ_y	σ_x
9	Y2T	±55°	0	70
Ratio:0:1	Y12	±55°	0	104
9	Y2T	±55°	77	77
Ratio:1:1	Y12	±55°	202	202
9	Y12	±55°	281	0
Ratio:1:0	Y2C&3T	±55°	140	0
9	Y3T	±55°	0	−128
Ratio: 0:-1	Y2C	±55°	0	−183
	Y12	±55°	0	−104
9	Y3T	±55°	−158	−79
Ratio:-2:-1	Y1C	±55°	−706	−353
9	Y2T	±55°	−204	0
Ratio:-1:0	Y12	±55°	−209	0

Table 8
Damage modes in the stress–strain curves

Loading case	Laminate lay-up	Failure modes	Failed plies	Stress levels (MPa)	
				σ_x	σ_y
7	$[0/\pm45/90]_s$	Y2T	90°	0	224
		Y2T	±45°	0	592
		Y1T	0°	0	625
8	$[0/\pm45/90]_s$	Y2T	90°	132	264
		Y2T	±45°	203	406
		Y1T	0°	367	734
10	$[\pm55]_s$	Y12	±55°	0	281
11	$[\pm55]_s$	Y2T	±55°	82	164
		Y1T	±55°	414	828
12	$[0/90]_s$	Y2T	90°	78	0
		Y1T	0°	634	0
13	$[\pm45]_s$	Y2T	±45°	92	92
		Y1T	±45°	621	621
14	$[\pm45]_s$	Y12	±45°	0	75

curves for loading applied in the y-direction (σ_y:σ_x = 1:0) are shown in Fig. 14. In this case, the loading results in shear loading on the ply-level; thus, the laminate displays nonlinear behavior until failure. For the case where a biaxial load (σ_y:σ_x = 2:1) is applied (Fig. 15), the mechanical response is more linear until final fracture, although some nonlinearity (due to in-plane shearing) is evident near the point of ultimate failure.

The stress–strain curves for uniaxial tension (σ_y:σ_x = 0:1) of a $[0/90]_s$ E-glass/MY750 laminate (case 12) is shown in Fig. 16. The final load cases, stress-strain curves for the biaxial loading of [+45/-45]s laminates of E-glass/MY750 epoxy, are shown in Figs. 17 and 18. For case 13, where $\sigma_y = \sigma_x$, the strains in the x and y directions are equivalent so one curve is shown in Fig. 17. Fig. 18 shows that for case 14, where $\sigma_y = -\sigma_x$,

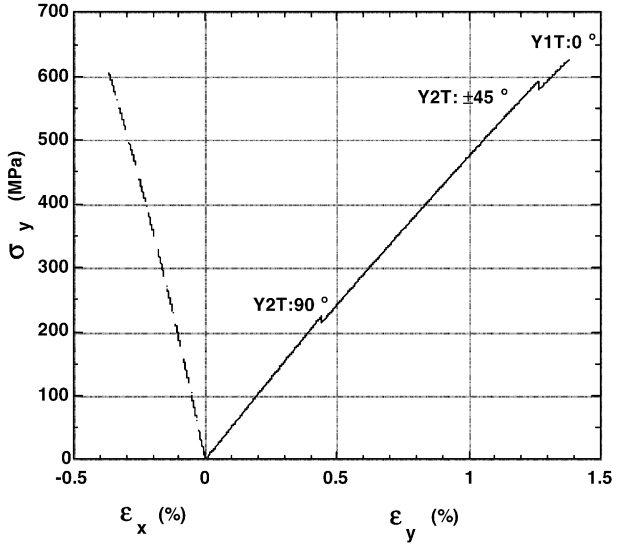

Fig. 12. Loading case 7: stress–strain curves (σ_y:σ_x = 1:0) and failure modes for [0/+45/−45/90]s AS4 graphite/3501-6 epoxy.

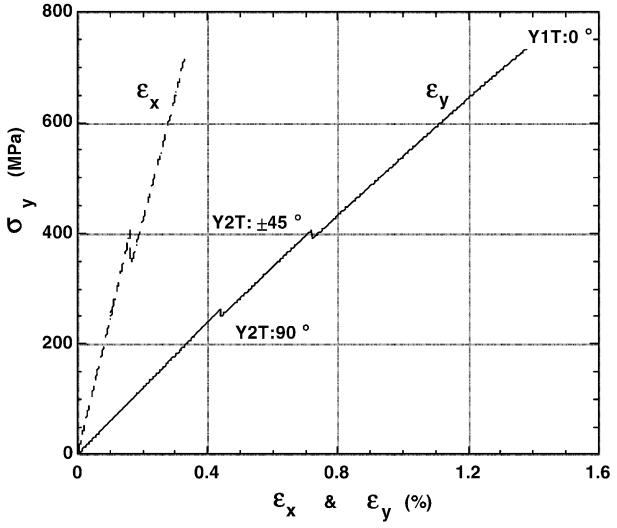

Fig. 13. Loading case 8: stress–strain curves (σ_y:σ_x = 2:1) and failure modes for [0/+45/−45/90]s AS4 graphite/3501-6 epoxy.

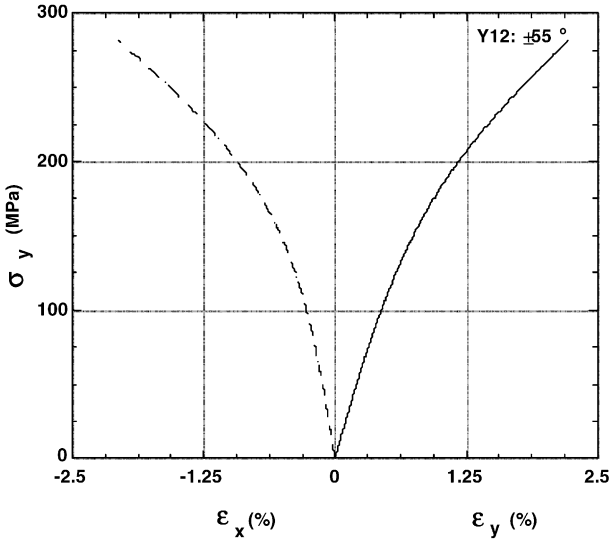

Fig. 14. Loading case 10: stress–strain curves (σ_y:σ_x = 1:0) and the final failure mode for [+55/−55]s E-glass/MY750 epoxy.

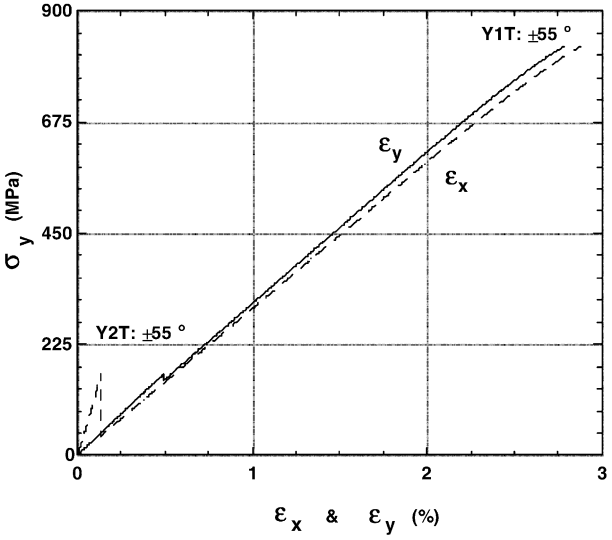

Fig. 15. Loading Case 11: stress–strain curves (σ_y:σ_x = 2:1) for [+55/−55]s E-glass/MY750 epoxy with the initial and final failure modes.

the strains are equal and opposite in the×and y directions, with both directions displaying significant nonlinear behavior.

Details of the progressive ply failures in loading cases 7–14 are summarized in Table 4. In particular, each level in loading where failure in a ply occurs is indicated. The associated ply and mode of failure for each failure load level are also given.

4. Conclusions

A methodology has been presented for predicting the nonlinear response and progressive failure of composite laminates. The predictions are based on an incremental formulation of a well-established three-dimensional laminated media analysis [2] coupled with a progressive ply failure methodology. Nonlinear lamina constitutive relations for the composite are represented using the Ramberg–Osgood equation [3]. Piece-wise linear increments in laminate stress and strain are calculated and superimposed to formulate the overall effective nonlinear response. Individual ply stresses and strains are monitored to calculate instantaneous ply stiffnesses for the incremental solution and to establish ply failure levels. The progressive-ply failure approach is used to allow for stress unloading in a ply and discrimination of the various potential modes of failure.

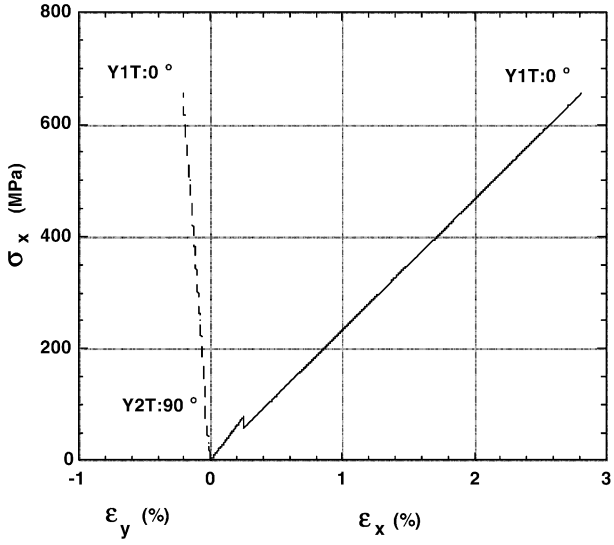

Fig. 16. Loading case 12: stress–strain curves (σ_y:σ_x = 0:1) for [0/90]s E-glass/MY750 epoxy with the initial and final failure modes.

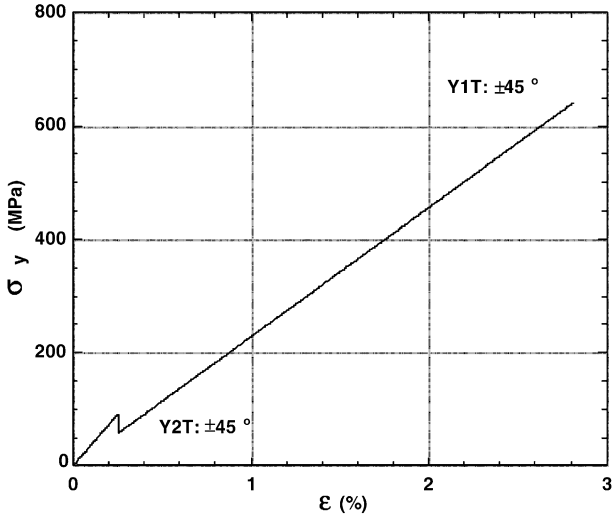

Fig. 17. Loading case 13: stress–strain curve (σ_y:σ_x = 1:1) for [+45/−45]s E-glass/MY750 epoxy with the initial and final failure modes.

The laminate response predictive capability presented in this paper is unique in relation to other existing capabilities. By adopting the three-dimensional laminated media theory, we are able to capture through-the-thickness effects in laminate response, which is particularly important for thick laminate analysis, where interlaminar loads may be of concern. The theory presented in this work is easily adapted for implementation in the design and failure assessment of composite structures. Employing the three-dimensional laminate analysis presented here and the widely accepted "smearing-unsmearing" approach [2], the authors have developed a computer software code, LAMPAT [32], that is particularly useful for the analysis and design of thick-section composite structures.

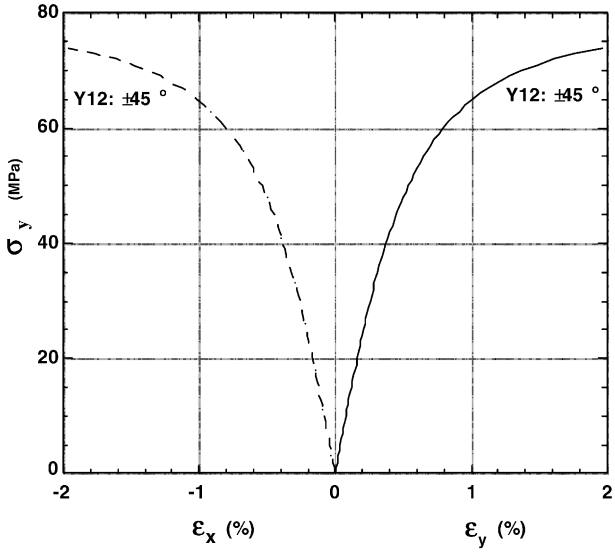

Fig. 18. Loading case 14: stress–strain curves (σ_y:σ_x = 1:-1) for [+45/−45]s E-glass/MY750 epoxy with the final failure fode.

In this paper, we have presented our prediction for biaxial failure envelopes and stress–strain curves for 14 different cases originally proposed by Hinton, Soden and Kaddour, Refs. [1,21]. The cases include prediction of the effective nonlinear stress-vs.-strain responses of laminates as well as initial and final ply failure envelop predictions. Comparison of these predictions with the actual experimental data will be made in a companion paper, Ref. [34], in Part C of the Worldwide Failure Olympics Exercise.

Uncited table

Table 8

Appendix. Lamina stiffness matrix coefficients

In this Appendix the lamina stiffness matrix coefficients are defined in terms of the lamina engineering constants and ply orientations. In the following descriptions, the primed notation will be used to denote the principal material coordinate system while the barred notation will be used to denote the global material coordinate system. By definition, the three-dimensional Hooke's Law linear-elastic stress–strain constitutive relation for an individual lamina is written in the following contracted form

$$\sigma_i'^k = C'_{ij}k\epsilon_j'^k \quad \text{for } (i,j = 1,2,3,4,5,6) \tag{A1}$$

where C'^k_{ij} represents the lamina stiffness matrix defined in the principal material coordinate system. The orthotropic lamina stiffness matrix is symmetric (i.e.,

$C'^{k}_{ij} = C'^{k}_{ji}$ for $i, j = 1, 2, 3, 4, 5, 6$) and takes the following form [33]

$$C'_{ij}k = \begin{bmatrix} C'_{11} & C'_{12} & C'_{13} & 0 & 0 & 0 \\ C'_{12} & C'_{22} & C'_{23} & 0 & 0 & 0 \\ C'_{13} & C'_{23} & C'_{33} & 0 & 0 & 0 \\ 0 & 0 & 0 & C'_{44} & 0 & 0 \\ 0 & 0 & 0 & 0 & C'_{55} & 0 \\ 0 & 0 & 0 & 0 & 0 & C'_{66} \end{bmatrix} \tag{A2}$$

The non-zero stiffness coefficients of the lamina stiffness matrix coefficients are defined in terms of the lamina engineering constants according to

$$\begin{aligned} C'_{11} &= \left(1 - \nu_{23}^2 E_3/E_2\right)E_1/V \\ C'_{12} &= (\nu_{12} + \nu_{13}\nu_{23}E_3/E_2)E_2/V \\ C'_{13} &= (\nu_{13} + \nu_{12}\nu_{23})E_3/V \\ C'_{22} &= \left(1 - \nu_{13}^2 E_3/E_1\right)\ E_2/V \\ C'_{23} &= (\nu_{23} - \nu_{12}\nu_{13}E_2/E_1)E_3/V \\ C'_{33} &= \left(1 - \nu_{12}^2 E_2/E_1\right)E_3/V \\ C'_{44} &= G_{23} \\ C'_{55} &= G_{13} \\ C'_{66} &= G_{12} \end{aligned} \tag{A3}$$

where

$$V = 1 - \nu_{12}(\nu_{12}E_2/E_1 + 2\nu_{23}\nu_{13}E_3/E_1) - \nu_{13}^2 E_3/E_1 - \nu_{23}^2 E_3/E_2$$

To define lamina stiffness coefficients in the global laminate system, transformation matrices for ply stress and ply strain between the principal (1, 2, 3) and global (x,y,z) coordinate systems is first considered. The global (barred) ply stresses, $\bar{\sigma}_i^k$, can be expressed explicitly in terms of the principal ply stresses, σ'^{k}_{i}, and the ply orientation angle, θ (see Fig. 1). Mathematically, this transformation is accomplished with the following second-order tensor transformation

$$\bar{\sigma}_i^k [T(\theta)]_{ij}^{\sigma} \sigma'^{k}_{j} \tag{A4}$$

where the stress transformation matrix is given by

$$[T(\theta)]_{ij}^{\sigma} = \begin{bmatrix} m^2 & n^2 & 0 & 0 & 0 & 2mn \\ n^2 & m^2 & 0 & 0 & 0 & -2mn \\ 0 & 0 & 1 & 0 & 0 & 0 \\ 0 & 0 & 0 & m & -n & 0 \\ 0 & 0 & 0 & n & m & 0 \\ -mn & mn & 0 & 0 & 0 & \left(m^2 - n^2\right) \end{bmatrix} \tag{A5}$$

and where $m = \cos\theta$ and $n = \sin\theta$. Similarly, global ply strains are obtained according to

$$\bar{\varepsilon}_i^k = [T(\theta)]_{ij}^{\varepsilon} \varepsilon'^{k}_{j} \tag{A6}$$

where the strain transformation matrix is given by

$$[T(\theta)]_{ij}^{\varepsilon} = \begin{bmatrix} m^2 & n^2 & 0 & 0 & 0 & -mn \\ n^2 & m^2 & 0 & 0 & 0 & mn \\ 0 & 0 & 1 & 0 & 0 & 0 \\ 0 & 0 & 0 & m & -n & 0 \\ 0 & 0 & 0 & n & m & 0 \\ -2mn & 2mn & 0 & 0 & 0 & \left(m^2 - n^2\right) \end{bmatrix} \tag{A7}$$

The lamina stress–strain constitutive relationship, defined in the global (x,y,z) laminate coordinate system, is written explicitly as

$$\bar{\sigma}_j^k = \bar{C}_{ij}^k \bar{\varepsilon}_j^k \text{for } (i, j = 1, 2, 3, 4, 5, 6). \tag{A8}$$

Combinding Eqs. (A1)–(A8), it can be shown that the lamina stiffness matrix elements, $\bar{C}_{ij}^k$, can be expressed explicitly in terms of the principal lamina stiffness matrix elements and the ply orientation angle, θ, through the following expression

$$\bar{C}_{ij}^k = [T(\theta)]_{ij}^{\theta} C'_{ij}k \left\{[T(\theta)]_{ij}^{\varepsilon}\right\}^{-1} \tag{A9}$$

Through Eqs. (A3),(A5),(A7) and (A9), the lamina stiffness matrix elements can be explicitly expressed in terms of the lamina engineering constants and ply orientations.

References

[1] Hinton MJ, Soden PD. Predicting failure in composite laminates: background to the exercise. Compos Sci Technol 1998;58(7):1001.

[2] Chou PC, Carleone J, Hsu CM. Elastic constants of layered media. J Compos Materials 1972;6:80–93.

[3] Richard RM, Blacklock JR. Finite element analysis of inelastic structures. AIAA Journal 1969;7:432.

[4] Chamis CC. Failure criteria for filamentary composites. Testing and Design, ASTM STP 1996;490:336–460.

[5] Sandhu RS. A Survey of failure theories of isotropic and anisotropic materials. AFFDL-TR-72-71, AD756889, Air Force Flight Dynamics Laboratory, Wright-Patterson Air Force Base, OH, USA, 1972.

[6] Soni SR. A comparative study of failure envelopes in composite laminates. J Reinf Plast Compos 1983;2:34–42.

[7] Tsai SW. A survey of macroscopic failure criteria for composite materials. J Reinf Plast Compos 1984;3:40–62.

[8] Nahas MN. Survey of failure and post failure theories of laminated fibre reinforced composites. J Compos Technol Res 1986;8:138–53.

[9] Gotsis PK, Chamis CC, Minnetyan L. Prediction of composite laminate fracture: micromechanics and progressive fracture. Compos Sci Technol 1998;58(7):1137.

[10] Eckold GC. Failure criteria for use in the design environment. Compos Sci Technol 1998;58(7):1095.

[11] Edge EC. Stress based grant-sanders method for predicting failure of composite laminates. Compos Sci Technol 1998;58(7):1033.

[12] Mccartney LN. Predicting transverse crack formation in cross-ply laminate. Compos Sci Technol 1998;58(7):1069.

[13] Hart-Smith LJ. Predictions of the original and truncated max-

imum-strain failure models for certain fibrous composite laminates. Compos Sci Technol 1998;58(7):1151.
[14] Hart-Smith LJ. Predictions of a generalized maximum-shear-stress failure criterion for certain fibrous composite laminates. Compos Sci Technol 1998;58(7):1179.
[15] Puck A, Schurmann H. Failure analysis of FRP laminates by means of physically based phenomenological models. Compos Sci Technol 1998;58(7):1045.
[16] Rotem A. Prediction of laminate failure with the rotem failure criterion. Compos Sci Technol 1998;58(7):1083.
[17] Sun CT, Tao JX. Prediction of failure envelopes and stress/strain behavior of composite laminates. Compos Sci Technol 1998; 58(7):1125.
[18] Lui KS, Tsai SW. A progressive quadratic failure criterion for a laminate. Compos Sci Technol 1998;58(7):1123.
[19] Wolfe WE, Butalia TS. A strain-energy based failure criterion for nonlinear analysis of composite laminates subjected to biaxial loading. Compos Sci Technol 1998;58(7):1107.
[20] Zinoview P, Grigoriev SV, Labedeva OV, Tairova LR. Strength of multilayered composites. Compos Sci Technol 1998;58(7): 1209.
[21] Soden PD, Hinton MJ, Kaddour AS. Lamina properties, lay-up configuration and loading conditions for a range of fibre reinforced composite laminates. Compos Sci Technol 1998;58(7): 1011.
[22] Soden PD, Hinton MJ, Kaddour AS. A comparison of the predictive capabilities of current failure theories for composite laminates. Compos Sci Technol 1998;58(7):1225.
[23] Bogetti TA, Hoppel CPR, Drysdale WH. Three-dimensional effective property and strength prediction of thick laminated composite media. ARL-TR-911, US Army Research Laboratory, Aberdeen Proving Ground, MD, October 1995.
[24] White JE, Angona FA. Elastic wave velocities in laminated media. J Acous Soc Am 1955;27:311.
[25] Postma GW. Wave propogation in a stratified medium. Geophysics 1955;20:780.
[26] Rytov SM. Acoustical properties of a thinly laminated medium. Soviet Phys Acoustics 1956;2:68.
[27] Behrens E. Sound propagation in lamellar composite materials and averaged elastic constants. J Acous Soc Am 1967;42:378.
[28] Salamon MDG. Elastic moduli of stratified rock mass. Int J Rock Mech Min Sci 1968:519.
[29] Sun CT, Liao WC. Analysis of thick section composite laminates using effective moduli. J Compos Materials 1990;24:977.
[30] Vinson JR, Sierakowski RL. The behavior of structures composed of composite materials. Dordrecht, The Netherlands: Martinus Nijhoff Publishers; 1986.
[31] Hoppel CPR, DeTeresa SJ. Effect of angle-ply orientation on compression strength of composite laminates. US Army Symposium on Solid Mechanics Proceedings, Myrtle Beach, SC 14 April 1999.
[32] Bogetti TA, Hoppel CPR, Burns BP. LAMPAT: a software tool for the analysis and design of thick laminated composite structures. US Army Research Laboratory Technical Report, ARL-TR-890, September, 1995.
[33] Whitney JM. Structural analysis of laminated anisotropic plates. Lancaster, PA: Technomic Publishing Co; 1987.
[34] Bogetti TA, Hoppel CPR, Harik VM, Newill JF, Burns BP. Predicting the nonlinear response and failure of composite laminates: correlation with experimental results. Compos Sci Technol [in press].

NO. OF COPIES	ORGANIZATION
1 (PDF Only)	DEFENSE TECHNICAL INFORMATION CTR DTIC OCA 8725 JOHN J KINGMAN RD STE 0944 FT BELVOIR VA 22060-6218
1	COMMANDING GENERAL US ARMY MATERIEL CMD AMCRDA TF 5001 EISENHOWER AVE ALEXANDRIA VA 22333-0001
1	INST FOR ADVNCD TCHNLGY THE UNIV OF TEXAS AT AUSTIN 3925 W BRAKER LN STE 400 AUSTIN TX 78759-5316
1	US MILITARY ACADEMY MATH SCI CTR EXCELLENCE MADN MATH THAYER HALL WEST POINT NY 10996-1786
1	DIRECTOR US ARMY RESEARCH LAB AMSRD ARL CS IS R 2800 POWDER MILL RD ADELPHI MD 20783-1197
3	DIRECTOR US ARMY RESEARCH LAB AMSRD ARL CI OK TL 2800 POWDER MILL RD ADELPHI MD 20783-1197
3	DIRECTOR US ARMY RESEARCH LAB AMSRD ARL CS IS T 2800 POWDER MILL RD ADELPHI MD 20783-1197

NO. OF COPIES	ORGANIZATION
	ABERDEEN PROVING GROUND
1	DIR USARL AMSRD ARL CI OK TP (BLDG 4600)

NO. OF COPIES ORGANIZATION

1 DIRECTOR
US ARMY RESEARCH LAB
AMSRD ARL SE L
D SNIDER
2800 POWDER MILL RD
ADELPHI MD 20783-1197

3 DIRECTOR
US ARMY RESEARCH LAB
AMSRD ARL OP SD TL
2800 POWDER MILL RD
ADELPHI MD 20783-1197

1 DIRECTOR
US ARMY RESEARCH LAB
AMSRD ARL SE R
H WALLACE
2800 POWDER MILL RD
ADELPHI MD 20783-1197

2 DIRECTOR
US ARMY RESEARCH LAB
AMSRD ARL SS SE DS
R REYZER
R ATKINSON
2800 POWDER MILL RD
ADELPHI MD 20783-1197

7 DIRECTOR
US ARMY RESEARCH LAB
AMSRD ARL WM MB
A ABRAHAMIAN
M BERMAN
M CHOWDHURY
A FRYDMAN
T LI
W MCINTOSH
E SZYMANSKI
2800 POWDER MILL RD
ADELPHI MD 20783-1197

1 COMMANDER
US ARMY MATERIEL CMD
AMXMI INT
5001 EISENHOWER AVE
ALEXANDRIA VA 22333-0001

NO. OF COPIES ORGANIZATION

3 COMMANDER
US ARMY ARDEC
AMSTA AR CC
M PADGETT
J HEDDERICH
H OPAT
PICATINNY ARSENAL NJ
07806-5000

2 COMMANDER
US ARMY ARDEC
AMSTA AR AE WW
E BAKER
J PEARSON
PICATINNY ARSENAL NJ
07806-5000

1 COMMANDER
US ARMY ARDEC
AMSTA AR FSE
PICATINNY ARSENAL NJ
07806-5000

1 COMMANDER
US ARMY ARDEC
AMSTA AR TD
PICATINNY ARSENAL NJ
07806-5000

13 COMMANDER
US ARMY ARDEC
AMSTA AR CCH A
F ALTAMURA
M NICOLICH
M PALATHINGUL
D VO
R HOWELL
A VELLA
M YOUNG
L MANOLE
S MUSALLI
R CARR
M LUCIANO
E LOGSDEN
T LOUZEIRO
PICATINNY ARSENAL NJ
07806-5000

NO. OF COPIES	ORGANIZATION
1	COMMANDER US ARMY ARDEC AMSTA AR CCH P J LUTZ PICATINNY ARSENAL NJ 07806-5000
1	COMMANDER US ARMY ARDEC AMSTA AR FSF T C LIVECCHIA PICATINNY ARSENAL NJ 07806-5000
1	COMMANDER US ARMY ARDEC AMSTA ASF PICATINNY ARSENAL NJ 07806-5000
1	COMMANDER US ARMY ARDEC AMSTA AR QAC T C J PAGE PICATINNY ARSENAL NJ 07806-5000
1	COMMANDER US ARMY ARDEC AMSTA AR M D DEMELLA PICATINNY ARSENAL NJ 07806-5000
3	COMMANDER US ARMY ARDEC AMSTA AR FSA A WARNASH B MACHAK M CHIEFA PICATINNY ARSENAL NJ 07806-5000
2	COMMANDER US ARMY ARDEC AMSTA AR FSP G M SCHIKSNIS D CARLUCCI PICATINNY ARSENAL NJ 07806-5000

NO. OF COPIES	ORGANIZATION
2	COMMANDER US ARMY ARDEC AMSTA AR CCH C H CHANIN S CHICO PICATINNY ARSENAL NJ 07806-5000
1	COMMANDER US ARMY ARDEC AMSTA AR QAC T D RIGOGLIOSO PICATINNY ARSENAL NJ 07806-5000
1	COMMANDER US ARMY ARDEC AMSTA AR WET T SACHAR BLDG 172 PICATINNY ARSENAL NJ 07806-5000
1	US ARMY ARDEC INTELLIGENCE SPECIALIST AMSTA AR WEL F M GUERRIERE PICATINNY ARSENAL NJ 07806-5000
10	COMMANDER US ARMY ARDEC AMSTA AR CCH B P DONADIA F DONLON P VALENTI C KNUTSON G EUSTICE K HENRY J MCNABOC G WAGNECZ R SAYER F CHANG PICATINNY ARSENAL NJ 07806-5000

NO. OF COPIES	ORGANIZATION
6	COMMANDER US ARMY ARDEC AMSTA AR CCL F PUZYCKI R MCHUGH D CONWAY E JAROSZEWSKI R SCHLENNER M CLUNE PICATINNY ARSENAL NJ 07806-5000
1	PM ARMS SFAE GCSS ARMS BLDG 171 PICATINNY ARSENAL NJ 07806-5000
1	COMMANDER US ARMY ARDEC AMSTA AR WEA J BRESCIA PICATINNY ARSENAL NJ 07806-5000
1	PM MAS SFAE AMO MAS PICATINNY ARSENAL NJ 07806-5000
1	PM MAS SFAE AMO MAS CHIEF ENGINEER PICATINNY ARSENAL NJ 07806-5000
1	PM MAS SFAE AMO MAS PS PICATINNY ARSENAL NJ 07806-5000
2	PM MAS SFAE AMO MAS LC PICATINNY ARSENAL NJ 07806-5000
2	PM MAS SFAE AMO MAS MC PICATINNY ARSENAL NJ 07806-5000

NO. OF COPIES	ORGANIZATION
1	COMMANDER US ARMY ARDEC PRODUCTION BASE MODERN ACTY AMSMC PBM K PICATINNY ARSENAL NJ 07806-5000
1	COMMANDER US ARMY TACOM PM COMBAT SYSTEMS SFAE GCS CS 6501 ELEVEN MILE RD WARREN MI 48397-5000
1	COMMANDER US ARMY TACOM AMSTA SF WARREN MI 48397-5000
1	DIRECTOR AIR FORCE RESEARCH LAB MLLMD D MIRACLE 2230 TENTH ST WRIGHT PATTERSON AFB OH 45433-7817
1	OFC OF NAVAL RESEARCH J CHRISTODOULOU ONR CODE 332 800 N QUINCY ST ARLINGTON VA 22217-5600
1	US ARMY CERL R LAMPO 2902 NEWMARK DR CHAMPAIGN IL 61822
1	COMMANDER US ARMY TACOM PM SURVIVABLE SYSTEMS SFAE GCSS W GSI H M RYZYI 6501 ELEVEN MILE RD WARREN MI 48397-5000

NO. OF COPIES	ORGANIZATION
1	COMMANDER US ARMY TACOM CHIEF ABRAMS TESTING SFAE GCSS W AB QT T KRASKIEWICZ 6501 ELEVEN MILE RD WARREN MI 48397-5000
1	COMMANDER WATERVLIET ARSENAL SMCWV QAE Q B VANINA BLDG 44 WATERVLIET NY 12189-4050
1	TNG, DOC, & CBT DEV ATZK TDD IRSA A POMEY FT KNOX KY 40121
2	HQ IOC TANK AMMUNITION TEAM AMSIO SMT R CRAWFORD W HARRIS ROCK ISLAND IL 61299-6000
2	COMMANDER US ARMY AMCOM AVIATION APPLIED TECH DIR J SCHUCK FT EUSTIS VA 23604-5577
1	NSWC DAHLGREN DIV CODE G06 DAHLGREN VA 22448
2	US ARMY CORPS OF ENGR CERD C T LIU CEW ET T TAN 20 MASSACHUSETTS AVE NW WASHINGTON DC 20314
1	US ARMY COLD REGIONS RSCH & ENGRNG LAB P DUTTA 72 LYME RD HANOVER NH 03755

NO. OF COPIES	ORGANIZATION
14	COMMANDER US ARMY TACOM AMSTA TR R R MCCLELLAND D THOMAS J BENNETT D HANSEN AMSTA JSK S GOODMAN J FLORENCE K IYER D TEMPLETON A SCHUMACHER AMSTA TR D D OSTBERG L HINOJOSA B RAJU AMSTA CS SF H HUTCHINSON F SCHWARZ WARREN MI 48397-5000
14	BENET LABS AMSTA AR CCB R FISCELLA M SOJA E KATHE M SCAVULO G SPENCER P WHEELER S KRUPSKI J VASILAKIS G FRIAR R HASENBEIN AMSTA CCB R S SOPOK E HYLAND D CRAYON R DILLON WATERVLIET NY 12189-4050
1	USA SBCCOM PM SOLDIER SPT AMSSB PM RSS A J CONNORS KANSAS ST NATICK MA 01760-5057
1	NSWC TECH LIBRARY CODE 323 17320 DAHLGREN RD DAHLGREN VA 22448

NO. OF COPIES ORGANIZATION

2 USA SBCCOM
MATERIAL SCIENCE TEAM
AMSSB RSS
J HERBERT
M SENNETT
KANSAS ST
NATICK MA 01760-5057

2 OFC OF NAVAL RESEARCH
D SIEGEL CODE 351
J KELLY
800 N QUINCY ST
ARLINGTON VA 22217-5660

1 NSWC
CRANE DIVISION
M JOHNSON CODE 20H4
LOUISVILLE KY 40214-5245

2 NSWC
U SORATHIA
C WILLIAMS CD 6551
9500 MACARTHUR BLVD
WEST BETHESDA MD 20817

2 COMMANDER
NSWC
CARDEROCK DIVISION
R PETERSON CODE 2020
M CRITCHFIELD CODE 1730
BETHESDA MD 20084

8 DIRECTOR
US ARMY NGIC
D LEITER MS 404
M HOLTUS MS 301
M WOLFE MS 307
S MINGLEDORF MS 504
J GASTON MS 301
W GSTATTENBAUER MS 304
R WARNER MS 305
J CRIDER MS 306
2055 BOULDERS RD
CHARLOTTESVILLE VA
22911-8318

1 NAVAL SEA SYSTEMS CMD
D LIESE
1333 ISAAC HULL AVE SE 1100
WASHINGTON DC 20376-1100

NO. OF COPIES ORGANIZATION

1 EXPEDITIONARY WARFARE
DIV N85
F SHOUP
2000 NAVY PENTAGON
WASHINGTON DC 20350-2000

8 US ARMY SBCCOM
SOLDIER SYSTEMS CENTER
BALLISTICS TEAM
J WARD
W ZUKAS
P CUNNIFF
J SONG
MARINE CORPS TEAM
J MACKIEWICZ
BUS AREA ADVOCACY TEAM
W HASKELL
AMSSB RCP SS
W NYKVIST
S BEAUDOIN
KANSAS ST
NATICK MA 01760-5019

7 US ARMY RESEARCH OFC
A CROWSON
H EVERETT
J PRATER
G ANDERSON
D STEPP
D KISEROW
J CHANG
PO BOX 12211
RESEARCH TRIANGLE PARK NC
27709-2211

1 AFRL MLBC
2941 P ST RM 136
WRIGHT PATTERSON AFB OH
45433-7750

8 NSWC
J FRANCIS CODE G30
D WILSON CODE G32
R D COOPER CODE G32
J FRAYSSE CODE G33
E ROWE CODE G33
T DURAN CODE G33
L DE SIMONE CODE G33
R HUBBARD CODE G33
DAHLGREN VA 22448

NO. OF COPIES ORGANIZATION

1 NSWC
CARDEROCK DIVISION
R CRANE CODE 6553
9500 MACARTHUR BLVD
WEST BETHESDA MD 20817-5700

1 AFRL MLSS
R THOMSON
2179 12TH ST RM 122
WRIGHT PATTERSON AFB OH
45433-7718

2 AFRL
F ABRAMS
J BROWN
BLDG 653
2977 P ST STE 6
WRIGHT PATTERSON AFB OH
45433-7739

5 DIRECTOR
LLNL
R CHRISTENSEN
S DETERESA
F MAGNESS
M FINGER MS 313
M MURPHY L 282
PO BOX 808
LIVERMORE CA 94550

1 AFRL MLS OL
L COULTER
5851 F AVE
BLDG 849 RM AD1A
HILL AFB UT 84056-5713

1 DIRECTOR
LOS ALAMOS NATL LAB
F L ADDESSIO T 3 MS 5000
PO BOX 1633
LOS ALAMOS NM 87545

1 OSD
JOINT CCD TEST FORCE
OSD JCCD
R WILLIAMS
3909 HALLS FERRY RD
VICKSBURG MS 29180-6199

1 OAK RIDGE NATL LAB
C EBERLE MS 8048
PO BOX 2008
OAK RIDGE TN 37831

NO. OF COPIES ORGANIZATION

3 DARPA
M VANFOSSEN
S WAX
L CHRISTODOULOU
3701 N FAIRFAX DR
ARLINGTON VA 22203-1714

2 SERDP PROGRAM OFC
PM P2
C PELLERIN
B SMITH
901 N STUART ST STE 303
ARLINGTON VA 22203

1 OAK RIDGE NATL LAB
R M DAVIS
PO BOX 2008
OAK RIDGE TN 37831-6195

3 DIRECTOR
SANDIA NATL LABS
APPLIED MECHS DEPT
MS 9042
J HANDROCK
Y R KAN
J LAUFFER
PO BOX 969
LIVERMORE CA 94551-0969

1 OAK RIDGE NATL LAB
C D WARREN MS 8039
PO BOX 2008
OAK RIDGE TN 37831

4 NIST
M VANLANDINGHAM MS 8621
J CHIN MS 8621
J MARTIN MS 8621
D DUTHINH MS 8611
100 BUREAU DR
GAITHERSBURG MD 20899

1 HYDROGEOLOGIC INC
SERDP ESTCP SPT OFC
S WALSH
1155 HERNDON PKWY STE 900
HERNDON VA 20170

NO. OF COPIES ORGANIZATION

3 NASA LANGLEY RESEARCH CTR
AMSRD ARL VS
W ELBER MS 266
F BARTLETT JR MS 266
G FARLEY MS 266
HAMPTON VA 23681-0001

1 NASA LANGLEY RESEARCH CTR
T GATES MS 188E
HAMPTON VA 23661-3400

1 FHWA
E MUNLEY
6300 GEORGETOWN PIKE
MCLEAN VA 22101

1 USDOT FEDERAL RAILROAD
M FATEH RDV 31
WASHINGTON DC 20590

3 CYTEC FIBERITE
R DUNNE
D KOHLI
R MAYHEW
1300 REVOLUTION ST
HAVRE DE GRACE MD 21078

1 DIRECTOR
NGIC
IANG TMT
2055 BOULDERS RD
CHARLOTTESVILLE VA
22911-8318

1 SIOUX MFG
B KRIEL
PO BOX 400
FT TOTTEN ND 58335

2 3TEX CORP
A BOGDANOVICH
J SINGLETARY
109 MACKENAN DR
CARY NC 27511

1 3M CORP
J SKILDUM
3M CENTER BLDG 60 IN 01
ST PAUL MN 55144-1000

NO. OF COPIES ORGANIZATION

1 DIRECTOR
DEFENSE INTLLGNC AGNCY
TA 5
K CRELLING
WASHINGTON DC 20310

1 ADVANCED GLASS FIBER YARNS
T COLLINS
281 SPRING RUN LANE STE A
DOWNINGTON PA 19335

1 COMPOSITE MATERIALS INC
D SHORTT
19105 63 AVE NE
PO BOX 25
ARLINGTON WA 98223

1 JPS GLASS
L CARTER
PO BOX 260
SLATER RD
SLATER SC 29683

1 COMPOSITE MATERIALS INC
R HOLLAND
11 JEWEL CT
ORINDA CA 94563

1 COMPOSITE MATERIALS INC
C RILEY
14530 S ANSON AVE
SANTA FE SPRINGS CA 90670

2 SIMULA
J COLTMAN
R HUYETT
10016 S 51ST ST
PHOENIX AZ 85044

2 PROTECTION MATERIALS INC
M MILLER
F CRILLEY
14000 NW 58 CT
MIAMI LAKES FL 33014

2 FOSTER MILLER
M ROYLANCE
W ZUKAS
195 BEAR HILL RD
WALTHAM MA 02354-1196

NO. OF COPIES	ORGANIZATION
1	ROM DEVELOPMENT CORP R O MEARA 136 SWINEBURNE ROW BRICK MARKET PLACE NEWPORT RI 02840
2	TEXTRON SYSTEMS T FOLTZ M TREASURE 1449 MIDDLESEX ST LOWELL MA 01851
1	O GARA HESS & EISENHARDT M GILLESPIE 9113 LESAINT DR FAIRFIELD OH 45014
2	MILLIKEN RESEARCH CORP H KUHN M MACLEOD PO BOX 1926 SPARTANBURG SC 29303
1	CONNEAUGHT INDUSTRIES INC J SANTOS PO BOX 1425 COVENTRY RI 02816
1	ARMTEC DEFENSE PRODUCTS S DYER 85 901 AVE 53 PO BOX 848 COACHELLA CA 92236
1	NATL COMPOSITE CTR T CORDELL 2000 COMPOSITE DR KETTERING OH 45420
3	PACIFIC NORTHWEST LAB M SMITH G VAN ARSDALE R SHIPPELL PO BOX 999 RICHLAND WA 99352
1	SAIC M PALMER 1410 SPRING HILL RD STE 400 MS SH4 5 MCLEAN VA 22102
8	ALLIANT TECHSYSTEMS INC C CANDLAND MN11 1428 C AAKHUS MN11 2830 B SEE MN11 2439 N VLAHAKUS MN11 2145 R DOHRN MN11 1428 S HAGLUND MN11 2439 M HISSONG MN11 2830 D KAMDAR MN11 2830 600 SECOND ST NE HOPKINS MN 55343-8367
1	R FIELDS 4680 OAKCREEK ST APT 206 ORLANDO FL 32835
1	APPLIED COMPOSITES W GRISCH 333 NORTH SIXTH ST ST CHARLES IL 60174
1	CUSTOM ANALYTICAL ENG SYS INC A ALEXANDER 13000 TENSOR LANE NE FLINTSTONE MD 21530
1	AAI CORP DR N B MCNELLIS PO BOX 126 HUNT VALLEY MD 21030-0126
1	OFC DEPUTY UNDER SEC DEFNS J THOMPSON 1745 JEFFERSON DAVIS HWY CRYSTAL SQ 4 STE 501 ARLINGTON VA 22202
3	ALLIANT TECHSYSTEMS INC J CONDON E LYNAM J GERHARD WV01 16 STATE RT 956 PO BOX 210 ROCKET CENTER WV 26726-0210

NO. OF COPIES	ORGANIZATION
1	HEXCEL INC R BOE PO BOX 18748 SALT LAKE CITY UT 84118
5	NORTHROP GRUMMAN B IRWIN K EVANS D EWART A SHREKENHAMER J MCGLYNN BLDG 160 DEPT 3700 1100 WEST HOLLYVALE ST AZUSA CA 91701
1	HERCULES INC HERCULES PLAZA WILMINGTON DE 19894
1	BRIGS COMPANY J BACKOFEN 2668 PETERBOROUGH ST HERNDON VA 22071-2443
1	ZERNOW TECHNICAL SERVICES L ZERNOW 425 W BONITA AVE STE 208 SAN DIMAS CA 91773
1	GENERAL DYNAMICS OTS L WHITMORE 10101 NINTH ST NORTH ST PETERSBURG FL 33702
2	GENERAL DYNAMICS OTS FLINCHBAUGH DIV K LINDE T LYNCH PO BOX 127 RED LION PA 17356
1	GKN WESTLAND AEROSPACE D OLDS 450 MURDOCK AVE MERIDEN CT 06450-8324
1	PRATT & WHITNEY C WATSON 400 MAIN ST MS 114 37 EAST HARTFORD CT 06108
5	SIKORSKY AIRCRAFT G JACARUSO T CARSTENSAN B KAY S GARBO MS S330A J ADELMANN 6900 MAIN ST PO BOX 9729 STRATFORD CT 06497-9729
1	AEROSPACE CORP G HAWKINS M4 945 2350 E EL SEGUNDO BLVD EL SEGUNDO CA 90245
2	CYTEC FIBERITE M LIN W WEB 1440 N KRAEMER BLVD ANAHEIM CA 92806
2	UDLP G THOMAS M MACLEAN PO BOX 58123 SANTA CLARA CA 95052
1	UDLP WARREN OFC A LEE 31201 CHICAGO RD SOUTH SUITE B102 WARREN MI 48093
2	UDLP R BRYNSVOLD P JANKE MS 170 4800 EAST RIVER RD MINNEAPOLIS MN 55421-1498
2	BOEING ROTORCRAFT P MINGURT P HANDEL 800 B PUTNAM BLVD WALLINGFORD PA 19086
1	LOCKHEED MARTIN SKUNK WORKS D FORTNEY 1011 LOCKHEED WAY PALMDALE CA 93599-2502

NO. OF COPIES ORGANIZATION

1 LOCKHEED MARTIN
R FIELDS
5537 PGA BLVD
SUITE 4516
ORLANDO FL 32839

1 NORTHRUP GRUMMAN CORP
ELECTRONIC SENSORS
& SYSTEMS DIV
E SCHOCH MS V 16
1745A W NURSERY RD
LINTHICUM MD 21090

1 GDLS DIVISION
D BARTLE
PO BOX 1901
WARREN MI 48090

2 GDLS
D REES
M PASIK
PO BOX 2074
WARREN MI 48090-2074

1 GDLS
MUSKEGON OPER
M SOIMAR
76 GETTY ST
MUSKEGON MI 49442

1 GENERAL DYNAMICS
AMPHIBIOUS SYS
SURVIVABILITY LEAD
G WALKER
991 ANNAPOLIS WAY
WOODBRIDGE VA 22191

6 INST FOR ADVANCED
TECH
H FAIR
I MCNAB
P SULLIVAN
S BLESS
W REINECKE
C PERSAD
3925 W BRAKER LN STE 400
AUSTIN TX 78759-5316

1 ARROW TECH ASSOC
1233 SHELBURNE RD STE D8
SOUTH BURLINGTON VT
05403-7700

NO. OF COPIES ORGANIZATION

1 R EICHELBERGER
CONSULTANT
409 W CATHERINE ST
BEL AIR MD 21014-3613

1 SAIC
G CHRYSSOMALLIS
8500 NORMANDALE LAKE BLVD
SUITE 1610
BLOOMINGTON MN 55437-3828

1 UCLA MANE DEPT ENGR IV
H T HAHN
LOS ANGELES CA 90024-1597

2 UNIV OF DAYTON
RESEARCH INST
R Y KIM
A K ROY
300 COLLEGE PARK AVE
DAYTON OH 45469-0168

1 UMASS LOWELL
PLASTICS DEPT
N SCHOTT
1 UNIVERSITY AVE
LOWELL MA 01854

1 IIT RESEARCH CTR
D ROSE
201 MILL ST
ROME NY 13440-6916

1 GA TECH RESEARCH INST
GA INST OF TCHNLGY
P FRIEDERICH
ATLANTA GA 30392

1 MICHIGAN ST UNIV
MSM DEPT
R AVERILL
3515 EB
EAST LANSING MI 48824-1226

1 UNIV OF WYOMING
D ADAMS
PO BOX 3295
LARAMIE WY 82071

1 PENN STATE UNIV
R S ENGEL
245 HAMMOND BLDG
UNIVERSITY PARK PA 16801

NO. OF COPIES ORGANIZATION

2 PENN STATE UNIV
R MCNITT
C BAKIS
212 EARTH ENGR
SCIENCES BLDG
UNIVERSITY PARK PA 16802

5 UNIV OF DELAWARE
CTR FOR COMPOSITE MTRLS
J GILLESPIE
M SANTARE
S YARLAGADDA
S ADVANI
D HEIDER
201 SPENCER LAB
NEWARK DE 19716

1 SOUTHWEST RESEARCH INST
ENGR & MATL SCIENCES DIV
J RIEGEL
6220 CULEBRA RD
PO DRAWER 28510
SAN ANTONIO TX 78228-0510

1 BATELLE NATICK OPERS
B HALPIN
313 SPEEN ST
NATICK MA 01760

3 DIRECTOR
US ARMY RESEARCH LAB
AMSRD ARL WM MB
A FRYDMAN
2800 POWDER MILL RD
ADELPHI MD 20783-1197

ABERDEEN PROVING GROUND

1 US ARMY ATC
CSTE DTC AT AC I
W C FRAZER
400 COLLERAN RD
APG MD 21005-5059

1 DIRECTOR
US ARMY RESEARCH LAB
AMSRD ARL OP AP L
APG MD 21005-5066

NO. OF COPIES ORGANIZATION

91 DIR USARL
AMSRD ARL CI
AMSRD ARL CS IO FI
M ADAMSON
AMSRD ARL SL BA
AMSRD ARL SL BL
D BELY
R HENRY
AMSRD ARL SL BG
AMSRD ARL WM
J SMITH
AMSRD ARL WM B
A HORST
T KOGLER
AMSRD ARL WM BA
D LYON
AMSRD ARL WM BC
J NEWILL
P PLOSTINS
A ZIELINSKI
AMSRD ARL WM BD
P CONROY
B FORCH
C LEVERITT
R PESCE RODRIGUEZ
B RICE
AMSRD ARL WM BE
M LEADORE
R LIEB
AMSRD ARL WM BF
S WILKERSON
AMSRD ARL WM BR
J BORNSTEIN
C SHOEMAKER
AMSRD ARL WM M
B FINK
J MCCAULEY
AMSRD ARL WM MA
L GHIORSE
S MCKNIGHT
E WETZEL
AMSRD ARL WM MB
J BENDER
T BOGETTI
L BURTON
R CARTER
K CHO
W DE ROSSET
G DEWING
R DOWDING
W DRYSDALE
R EMERSON
D HENRY

NO. OF COPIES	ORGANIZATION
	AMSRD ARL WM MB
	D HOPKINS
	R KASTE
	L KECSKES
	B POWERS
	D SNOHA
	J SOUTH
	M STAKER
	J SWAB
	J TZENG
	AMSRD ARL WM MC
	J BEATTY
	R BOSSOLI
	E CHIN
	S CORNELISON
	D GRANVILLE
	B HART
	J LASALVIA
	J MONTGOMERY
	F PIERCE
	E RIGAS
	W SPURGEON
	AMSRD ARL WM MD
	B CHEESEMAN
	P DEHMER
	R DOOLEY
	G GAZONAS
	S GHIORSE
	C HOPPEL
	M KLUSEWITZ
	W ROY
	J SANDS
	D SPAGNUOLO
	S WALSH
	S WOLF
	AMSRD ARL WM T
	B BURNS
	AMSRD ARL WM TA
	W BRUCHEY
	M BURKINS
	W GILLICH
	B GOOCH
	T HAVEL
	E HORWATH
	M NORMANDIA
	J RUNYEON
	M ZOLTOSKI
	AMSRD ARL WM TB
	P BAKER
	AMSRD ARL WM TC
	R COATES

NO. OF COPIES	ORGANIZATION
	AMSRD ARL WM TD
	D DANDEKAR
	T HADUCH
	T MOYNIHAN
	M RAFTENBERG
	S SCHOENFELD
	T WEERASOORIYA
	AMSRD ARL WM TE
	A NIILER
	J POWELL

INTENTIONALLY LEFT BLANK.